

Supporting Information

Elucidating the reduction behavior of sulfurized poly(acrylonitrile) (SPAN) in lithium-sulfur-batteries using a carbonate electrolyte: A computational study

S. V. Klostermann, J. Kappler, A. Waigum, M. R. Buchmeiser,
A. Köhn, and J. Kästner

Contents

1	Population Analysis	2
2	Sulfur Chain Splitting and Lithiation Investigations	4
2.1	Initial split Investigations	4
2.2	Lithiation Investigations and Li ⁺ Placements	4
2.3	Minimum Energy Structures	8
3	Redox Potential Calculations	9
4	Cartesian Coordinates of all Structures	9

1 Population Analysis

Figure S1 shows a graphical representation of the naming of the areas studied for population analysis. The detailed individual charges of the neutral and the charged model are shown in the Tables S1–S2 for each investigated functional and for MP2.

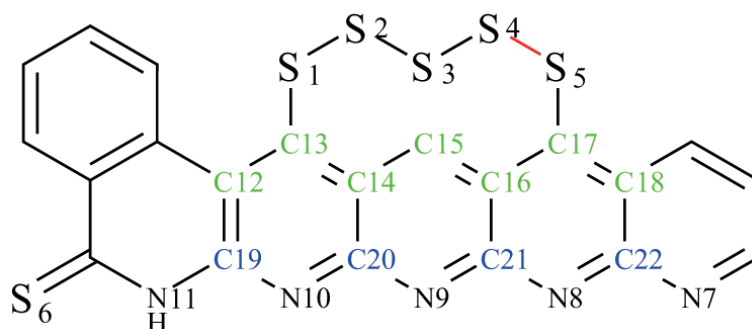


Figure S1: Indices for calculated population analyses. Green carbons: Carbons C, blue carbons: Carbons N, red line: investigated S-S bond.

Table S1: Differences in NBO charges for structures **0** to **2a** or **2b** for MP2, BP86-D3(BJ), and TPSSh-D3(BJ).

Atom Number	MP2			BP86-D3(BJ)			TPSSh-D3(BJ)		
	charges		Δ charges	charges		Δ charges	charges		Δ charges
	0	2a		0	2b		0	2b	
S 5	0.150	0.120	-0.030	0.129	-0.074	-0.203	0.131	-0.286	-0.416
S 4	0.011	-0.079	-0.090	-0.001	-0.211	-0.210	0.001	-0.570	-0.571
S 3	0.026	0.002	-0.024	0.021	0.167	0.147	0.017	0.061	0.044
S 2	-0.002	-0.066	-0.064	-0.014	-0.448	-0.434	-0.007	-0.154	-0.147
S 1	0.163	0.130	-0.033	0.143	-0.191	-0.334	0.142	-0.024	-0.166
S 6	-0.257	-0.458	-0.202	-0.110	-0.286	-0.175	-0.188	-0.275	-0.087
N 7	-0.620	-0.629	-0.009	-0.471	-0.504	-0.034	-0.519	-0.552	-0.033
N 8	-0.616	-0.718	-0.102	-0.453	-0.529	-0.076	-0.503	-0.609	-0.106
N 9	-0.649	-0.774	-0.125	-0.476	-0.527	-0.051	-0.528	-0.574	-0.046
N 10	-0.653	-0.717	-0.064	-0.501	-0.575	-0.074	-0.535	-0.572	-0.037
N 11	-0.661	-0.624	0.037	-0.538	-0.538	0.000	-0.548	-0.550	-0.002
C 12	-0.129	-0.179	-0.050	-0.084	-0.156	-0.072	-0.080	-0.129	-0.050
C 13	-0.063	-0.293	-0.230	-0.105	-0.133	-0.029	-0.095	-0.093	0.003
C 14	-0.202	-0.060	0.142	-0.112	-0.133	-0.021	-0.117	-0.148	-0.031
C 15	-0.031	-0.431	-0.400	-0.162	-0.148	0.014	-0.130	-0.104	0.026
C 16	-0.193	-0.040	0.153	-0.109	-0.131	-0.022	-0.114	-0.155	-0.040
C 17	-0.035	-0.339	-0.303	-0.095	-0.118	-0.022	-0.083	-0.107	-0.025
C 18	-0.184	-0.140	0.044	-0.123	-0.148	-0.026	-0.124	-0.172	-0.048
C 19	0.640	0.527	-0.114	0.475	0.448	-0.027	0.504	0.480	-0.024
C 20	0.589	0.588	-0.002	0.446	0.437	-0.009	0.468	0.456	-0.012
C 21	0.564	0.582	0.019	0.438	0.432	-0.006	0.457	0.452	-0.005
C 22	0.554	0.485	-0.069	0.434	0.416	-0.018	0.453	0.436	-0.017

Table S2: Differences in NBO charges for structures **0** to **2a** or **2b** for B3LYP-D3(BJ), M06, and cam-B3LYP.

Atom Number	B3LYP-D3(BJ)			M06			cam-B3LYP		
	charges		Δ charges	charges		Δ charges	charges		Δ charges
	0	2b		0	2a		0	2a	
S 5	0.134	-0.262	-0.396	0.135	0.081	-0.054	0.128	0.088	-0.040
S 4	-0.003	-0.589	-0.586	0.003	-0.113	-0.117	0.005	-0.110	-0.115
S 3	0.025	0.045	0.020	0.024	-0.035	-0.059	0.018	-0.030	-0.048
S 2	-0.003	-0.148	-0.145	0.002	-0.080	-0.082	-0.001	-0.069	-0.067
S 1	0.140	-0.019	-0.160	0.141	0.102	-0.038	0.137	0.104	-0.033
S 6	-0.176	-0.265	-0.089	-0.165	-0.358	-0.193	-0.190	-0.378	-0.188
N 7	-0.521	-0.554	-0.033	-0.546	-0.582	-0.037	-0.528	-0.563	-0.036
N 8	-0.510	-0.619	-0.110	-0.536	-0.644	-0.108	-0.513	-0.639	-0.127
N 9	-0.534	-0.581	-0.047	-0.563	-0.667	-0.104	-0.540	-0.667	-0.127
N 10	-0.542	-0.575	-0.033	-0.568	-0.635	-0.067	-0.550	-0.624	-0.074
N 11	-0.558	-0.558	0.000	-0.594	-0.583	0.011	-0.577	-0.557	0.019
C 12	-0.080	-0.132	-0.051	-0.085	-0.143	-0.058	-0.084	-0.150	-0.066
C 13	-0.091	-0.083	0.008	-0.088	-0.227	-0.138	-0.080	-0.225	-0.145
C 14	-0.119	-0.152	-0.033	-0.128	-0.093	0.035	-0.133	-0.084	0.048
C 15	-0.127	-0.101	0.025	-0.118	-0.314	-0.196	-0.115	-0.349	-0.234
C 16	-0.118	-0.156	-0.038	-0.126	-0.078	0.048	-0.128	-0.072	0.056
C 17	-0.073	-0.100	-0.027	-0.067	-0.295	-0.228	-0.067	-0.308	-0.241
C 18	-0.124	-0.174	-0.049	-0.132	-0.126	0.006	-0.130	-0.126	0.004
C 19	0.511	0.486	-0.025	0.537	0.465	-0.073	0.526	0.450	-0.076
C 20	0.472	0.460	-0.012	0.496	0.492	-0.005	0.481	0.482	0.000
C 21	0.461	0.458	-0.003	0.483	0.490	0.007	0.466	0.483	0.018
C 22	0.457	0.441	-0.016	0.478	0.433	-0.045	0.463	0.417	-0.046

Table S3: Differences in NBO charges for structures **0** to **2a** or **2b** for PBE0-D3(BJ) and PBEh-3c.

Atom Number	PBE0-D3(BJ)			PBEh-3c		
	charges		Δ charges	charges		Δ charges
	0	2a		0	2b	
S 5	0.137	0.093	-0.044	0.145	0.105	-0.040
S 4	0.003	-0.099	-0.103	0.006	-0.093	-0.098
S 3	0.021	-0.034	-0.056	0.020	-0.027	-0.047
S 2	-0.002	-0.075	-0.073	-0.001	-0.074	-0.073
S 1	0.145	0.109	-0.035	0.152	0.120	-0.032
S 6	-0.178	-0.387	-0.209	-0.184	-0.394	-0.211
N 7	-0.523	-0.564	-0.042	-0.549	-0.584	-0.035
N 8	-0.508	-0.619	-0.111	-0.536	-0.649	-0.114
N 9	-0.534	-0.643	-0.109	-0.563	-0.684	-0.120
N 10	-0.542	-0.617	-0.076	-0.570	-0.646	-0.076
N 11	-0.563	-0.553	0.010	-0.608	-0.588	0.021
C 12	-0.085	-0.139	-0.055	-0.093	-0.151	-0.058
C 13	-0.096	-0.240	-0.145	-0.100	-0.261	-0.161
C 14	-0.125	-0.097	0.028	-0.140	-0.091	0.049
C 15	-0.137	-0.325	-0.188	-0.117	-0.346	-0.228
C 16	-0.122	-0.087	0.034	-0.136	-0.076	0.060
C 17	-0.081	-0.286	-0.205	-0.084	-0.319	-0.235
C 18	-0.130	-0.132	-0.002	-0.140	-0.134	0.006
C 19	0.514	0.445	-0.069	0.547	0.466	-0.081
C 20	0.474	0.470	-0.003	0.503	0.506	0.002
C 21	0.462	0.467	0.006	0.488	0.502	0.014
C 22	0.458	0.416	-0.042	0.484	0.437	-0.047

Table S4: Single point energies for structures **0**, **2a**, **2b**, and **2c** in Hartree for different levels of theory.

Structure	Single point energies /Hartree				
	LCC	M06	cam-B3LYP	PBE0-D3(BJ)	PBEh-3c
0	-3464.5828	-3468.2408	-3468.5937	-3467.1320	-3464.8579
2a	-3464.8595	-3468.5193	-3468.8711	-3467.4135	-3465.1463
2b	-3464.8957	-3468.5477	-3468.9075	-3467.4341	-3465.1734
2c	-3464.8802	-3468.5316	-3468.8956	-3467.4201	-3465.1608

2 Sulfur Chain Splitting and Lithiation Investigations

2.1 Initial split Investigations

For the energetically most favorable splitting of the sulfur chain, energies of different splitting patterns were calculated. Structure **0** belongs to the neutral, uncharged SPAN model with non-split chain, **2b** has a 4-1 split chain with S_1 and S_4 sulfur chain residues and **2c** a 3-2 split sulfur chain with S_3 and S_2 sulfur chain residues.

Table S5: Investigated sulfur chain splitting patterns with their relative energies. Geometry optimizations at PBEh-3c/def2-mSVP level of theory. Single-point energies at cam-B3LYP/def2-TZVPD level of theory.

Structure	ZPE /a.u.	E_{elec} /a.u.	ΔE /eV	$\Delta E_{relative}$ /eV
0	0.2741	-3468.5937	0.000	
2a	0.2711	-3468.8711	-7.547	0.000
2b	0.2717	-3468.9075	-8.536	-0.989
2c	0.2713	-3468.8956	-8.213	-0.666

2.2 Lithiation Investigations and Li^+ Placements

The energy of electron and lithium cation addition was determined by calculating the individual steps and the concerted addition and comparing their energies relative to each other. The energies for the first and second lithiation are shown exemplarily in Table S6.

Table S6: Gibbs free energies of the respective systems with different order of steps with respect to the separated compounds **0** and Li^+ .

System	E_{elec} /Hartree	G(T) /Hartree	G_{total} /eV	$\Delta G_{rel.}$ /eV	Charge	Step
Li^+	-7.4024	-	-201.346	-	1	-
0	-3468.5937	0.2226	-94340.317	0.000	0	-
1_Li0	-3468.7433	0.2199	-94344.460	-4.143	-1	e-
0_Li1	-3476.0151	0.2224	-94542.186	-0.523	1	Li+
1_Li1	-3476.1838	0.2216	-94546.798	-5.135	0	Li+/e-
2_Li1	-3476.3744	0.2214	-94552.010	-10.346	-1	e-
1_Li2	-3483.5882	0.2203	-94748.234	-5.224	1	Li+
2_Li2	-3483.8176	0.2214	-94754.443	-11.434	0	Li+/e-
2_Li0	-3468.9075	0.2204	-94348.912	-8.595	-2	2e-

Based on the position of the spin density, the four positions for lithium cation placement can be identified in the following lithiations. The spin density is preferably localized at the ends of the free sulfur chains. Figure S2 shows the spin density distribution of structure **1_Li1**.

For each electron step, different Li^+ placements were investigated. Their relative energies to each other were examined. Four possible placement positions were distinguished:

- The 'between' position between the sulfur chain residues at the SPAN backbone. Marked as **_b** attached at the structure name.
- The 'middle' position in the middle of the longer sulfur chain residue. Marked as **_m** attached at the structure name.

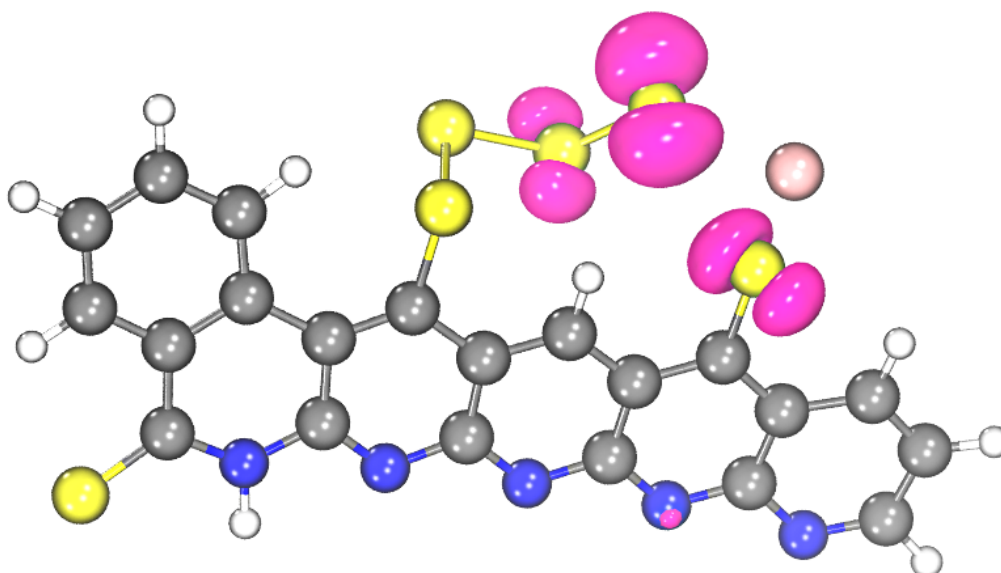


Figure S2: Calculated spin density (color: magenta) of structure **1_Li1** on the orbitals of the optimized geometry.

- The 'other' position on the other side of the backbone near the shorter sulfur chain residue. Marked as **_o** attached at the structure name.
- The 'end' position at the free end of the longer sulfur chain residue at the SPAN backbone. Marked as **_e** attached at the structure name.

The energetically favored placement, which was the between position for $n = 1$, was taken as the starting point for the next reduction step. Based on the optimized **1Li_b** structure, the four placement options were examined again for $n = 2$. The energetically best one was selected, see Table S7.

Table S7: Gibbs free energies of the four different possible Li^+ placements relative to each other in the respective electron step n .

System	E_{elec} /Hartree	$G(T)$ /Hartree	G_{total} /Hartree	$\Delta G_{\text{rel.}}$ /eV
Step $n = 1$				
1_Li1_b	-3476.1838	0.2216	-3475.9622	0.000
1_Li1_m	-3476.1756	0.2202	-3475.9554	0.187
1_Li1_o		moves to b		
1_Li1_e		moves to m		
Step $n = 2$				
2_Li2_b	-3483.8071	0.2207	-3483.5864	0.000
2_Li2_m	-3483.8143	0.2208	-3483.5935	-0.193
2_Li2_o	-3483.8140	0.2208	-3483.5932	-0.186
2_Li2_e	-3483.8176	0.2214	-3483.5962	-0.267

Figures S3–S8 show the structures of the steps $n = 1$ and $n = 2$ with different placements of Li^+ . All distances are given in Ångstrom. Color coding: grey= carbon, blue= nitrogen, yellow=sulfur, pink=lithium, white= hydrogen.

Nudged elastic band (NEB) path of the lithiation process from **2_Li2** to **3_Li3**. In the process, the lithium cation from the environment approaches and binds to the sulfur chain. The electron is delocalized on the SPAN backbone. A low barrier is visible.

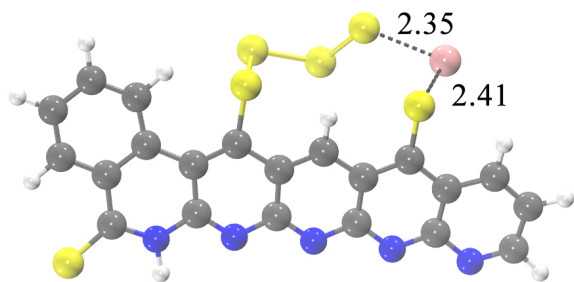


Figure S3: Structure **1_Li1_b** with one attached Li^+ at the 'between' position between the sulfur chain residues at the SPAN backbone.

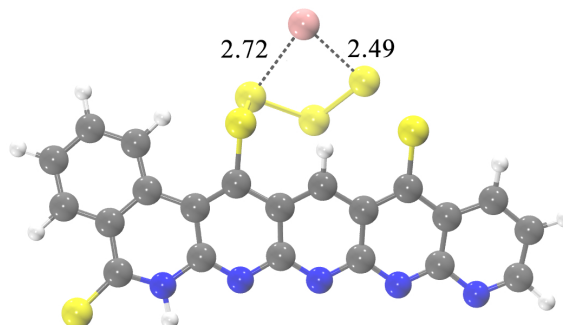


Figure S4: Structure **1_Li1_m** with the attached Li^+ at the 'middle' position in the middle of the longer sulfur chain residue at the SPAN backbone.

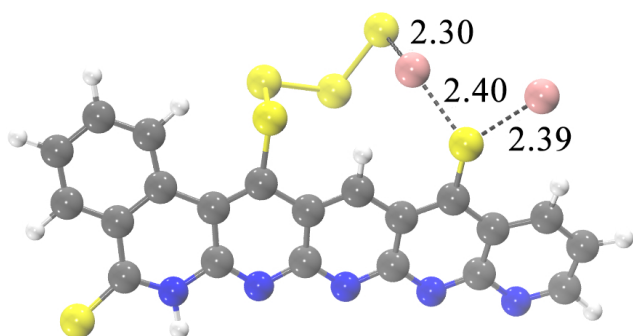


Figure S5: Structure **2_Li2_b** with the new attached Li^+ at the 'between' position between the sulfur chain residues at the SPAN backbone.

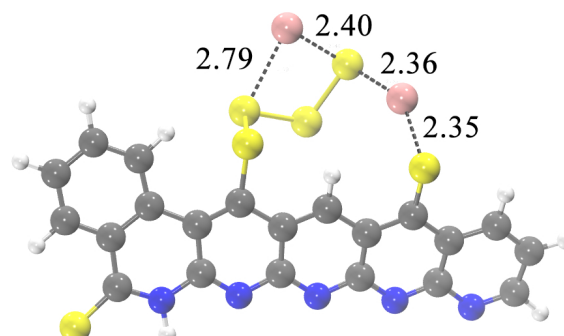


Figure S6: Structure **2_Li2_m** with the new attached Li^+ at the 'middle' position in the middle of the longer sulfur chain residue at the SPAN backbone.

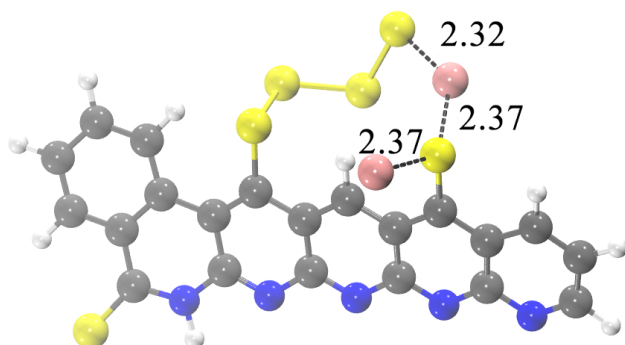


Figure S7: Structure **2_Li2_o** with the new attached Li^+ at the 'other' position on the other side of the backbone near the shorter sulfur chain residue at the SPAN backbone.

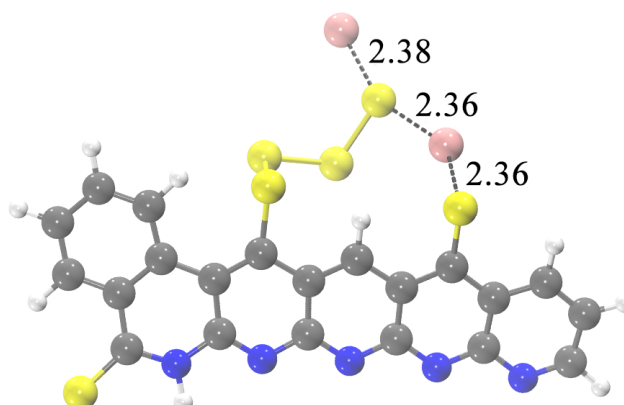


Figure S8: Structure **2_Li2_e** with the new attached Li^+ at the 'end' position at the free end of the longer sulfur chain residue at the SPAN backbone.

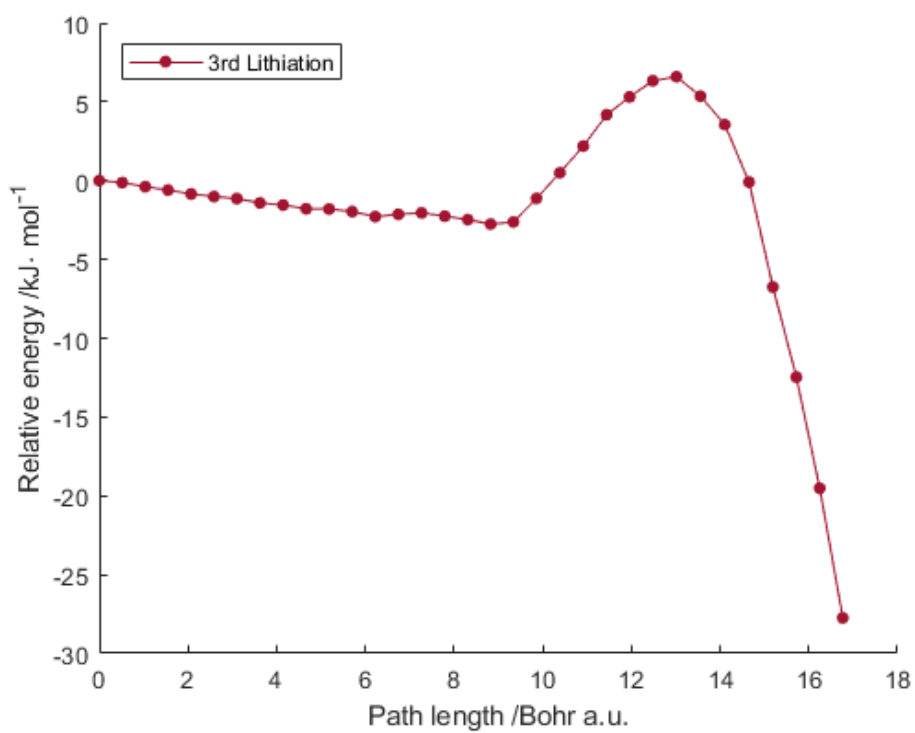


Figure S9: Calculated relative energy along the NEB path for the 3rd lithiation of SPAN. A path length of 0 corresponds to Li⁺ at a distance of 10.35 Å from **3_Li2**, while the path length at 16.8 Bohr corresponds to **3_Li3**.

2.3 Minimum Energy Structures

To discover the minimum energy structure at each electron step, we explore various potential pathways. Consequently, we assess the options of introducing a pair of a lithium cation and an electron, removing a Li_2S molecule, or performing both actions in a concerted manner.

Table S8: Relative Gibbs free energies for different possible reaction steps starting from $n = 2$ (2_Li2).

System	$E_{\text{elec}}/\text{Hartree}$	$G(\text{T})/\text{Hartree}$	$G_{\text{total}}/\text{eV}$	$G_{\text{rel.}}/\text{eV}$	Step
2_Li2	-3483.8176	0.2214	-94754.443	0.000	
2_Li0 + Li2S	-3483.6582	0.1972	-94750.765	3.678	Detachment
3_Li1 + Li2S	-3491.3429	0.1977	-94959.778	-3.989	Detachment + Li^+/e^-
3_Li3	-3491.3971	0.2195	-94960.659	-4.870	Li+/e-
3_Li3			-94960.659	0.000	
3_Li1 + Li2S	-3491.3425	0.1979	-94959.769	0.891	Detachment
4_Li2 + Li2S	-3498.9753	0.1983	-95167.364	-5.359	Detachment + Li^+/e^-
4_Li4	-3498.9539	0.2159	-95166.301	-4.296	Li+/e-
4_Li2 + Li2S	-3498.9753	0.1983	-95167.364	0.000	
4_Li0 + 2Li2S	-3498.8241	0.1729	-95163.943	3.421	Detachment
5_Li1 + 2Li2S	-3506.5054	0.1748	-95372.823	-4.113	Detachment + Li^+/e^-
5_Li3 Li2S	-3506.5565	0.1946	-95373.673	-4.963	Li+/e-

Table S9: Gibbs free energies of the respective minimum energy systems with different order of steps with respect to the separated compounds **1** and $\text{Li}^+/\text{Li}_2\text{S}$.

System	$E_{\text{elec}}/\text{Hartree}$	$G(\text{T})/\text{Hartree}$	$G_{\text{total}}/\text{Hartree}$	$G_{\text{total}}/\text{eV}$	$G_{\text{rel.}}/\text{eV}$
Li^+	-7.4024		-7.4024	-201.346	
Li_2S	-413.3824	-0.0232	-413.4056	-11244.708	
0	-3468.5937	0.2226	-3468.3711	-94340.317	0.000
1_Li1	-3476.1838	0.2208	-3475.9630	-94546.821	-5.135
2_Li2	-3483.8176	0.2214	-3483.5962	-94754.443	-11.434
3_Li3	-3491.3971	0.2187	-3491.1785	-94960.683	-16.304
4_Li2	-3085.5928	0.2730	-3085.3198	-83921.255	-21.663
5_Li3	-3093.1740	0.2212	-3092.9528	-84128.873	-26.626
6_Li2	-2687.3632	0.2207	-2687.1425	-73090.760	-31.784
7_Li3	-2694.9450	0.2176	-2694.7275	-73297.073	-36.720
8_Li2	-2289.1487	0.2186	-2288.9301	-62259.311	-42.326
9_Li3	-2296.7247	0.2166	-2296.5081	-62465.433	-47.111
10_Li2	-1890.8653	0.2169	-1890.6484	-51425.977	-51.029
11_Li3	-1898.4277	0.2145	-1898.2132	-51631.741	-55.447
12_Li2	-1492.5929	0.2169	-1492.3759	-40592.894	-59.962

3 Redox Potential Calculations

Fe(+II)/Fe(+III) and Cu(+II)/Cu(+III) references for redox potential calculations are shown in table S10.

Table S10: Calculated Gibbs free energies and absolute potentials of the redox systems Fe(+II)/Fe(+III) and Cu(+II)/Cu(+III).

System	Multiplicity	G(T) /Hartree	E _{elec} /Hartree	E _{total} /eV	E _{absolute} /V
Fe(+II)*18H ₂ O	5, high spin	0.3939	-2639.8473	-71793.607	0.000
Fe(+III)*18H ₂ O	6, high spin	0.3941	-2639.6387	-71787.927	5.681
Cu(+II)*18H ₂ O	2	0.3943	-3016.6034	-82041.431	0.000
Cu(+III)*18H ₂ O	3	0.3994	-3016.3269	-82033.770	7.660

Table S11: Redox potentials vs. Li/Li⁺ for the dominating species during the discharge mechanism.

Structure	E° (V vs. Li/Li ⁺)	
	Soluble Li ₂ S	Nucleated Li ₂ S
0	> 3.672	> 3.672
2_Li2	3.672	3.672
6_Li2	-	3.250
7_Li3	-	3.038
8_Li2	3.104	-
9_Li3	2.741	2.748
12_Li2	2.238	2.633

4 Cartesian Coordinates of all Structures

All optimized structures are provided in the file a11.xyz. Structure names with index **_a** indicate a structure with attached Li₂S molecule(s).